

Article

Opportunistic DF-AF Selection Relaying in Hybrid Wireless and Power Line Communication for Indoor IoT Networks

Hoang Thien Van ¹, Quyet-Nguyen Van ², Danh Hong Le ³, Hoang-Phuong Van ^{4,*}, Jakub Jalowiczor ⁵ , Hoang-Sy Nguyen ⁶  and Miroslav Voznak ⁵ 

¹ The Saigon International University (SIU), Ho Chi Minh City 700000, Vietnam; vanthienhoang@siu.edu.vn

² Faculty of Technology, Dong Nai Technology University, Dong Nai 760000, Vietnam; nguyenvanquyet@dntu.edu.vn

³ Van Hien University, Ho Chi Minh City 700000, Vietnam; danhlh@vhu.edu.vn

⁴ Faculty of Engineering and Technology, Thu Dau Mot University, Binh Duong 750000, Vietnam

⁵ Faculty of Electrical Engineering and Computer Science, VSB—Technical University of Ostrava, 17, Listopadu 2172/15, 708 00 Ostrava, Czech Republic; jakub.jalowiczor@vsb.cz (J.J.); miroslav.voznak@vsb.cz (M.V.)

⁶ Faculty of Information Technology, Robotics and Artificial Intelligence, Binh Duong University, Binh Duong 750000, Vietnam; nhsy@bdu.edu.vn

* Correspondence: phuongvh@tdmu.edu.vn



Citation: Van, H.T.; Van, Q.-N.; Le, D.H.; Van, H.-P.; Jalowiczor, J.; Nguyen, H.-S.; Voznak, M.

Opportunistic DF-AF Selection
Relaying in Hybrid Wireless and
Power Line Communication for
Indoor IoT Networks. *Sensors* **2021**,
21, 5469. <https://doi.org/10.3390/s21165469>

Academic Editor: Paolo Visconti

Received: 4 July 2021

Accepted: 1 August 2021

Published: 13 August 2021

Publisher's Note: MDPI stays neutral with regard to jurisdictional claims in published maps and institutional affiliations.



Copyright: © 2021 by the authors. Licensee MDPI, Basel, Switzerland. This article is an open access article distributed under the terms and conditions of the Creative Commons Attribution (CC BY) license (<https://creativecommons.org/licenses/by/4.0/>).

Abstract: This manuscript investigates the system performance of hybrid wireless and power line communication networks for indoor Internet of Things applications. Differentiating itself from the existing literature, the performance of the direct link and dual-hop energy harvesting relay-aided links is analyzed under the condition of indoor fading modeled by log-normal distribution. Moreover, the manuscript presents the analytical expressions of the successful transmission probability of the deployed opportunistic decode-and-forward and amplify-and-forward relay selection scheme, and validates them with Monte Carlo simulations. Moreover, the impact of different system parameters on the successful transmission probability is revealed. For the considered hybrid system, in general, the opportunistic decode-and-forward relaying scheme outperforms the opportunistic amplify-and-forward relaying scheme. As importantly, increasing the source to relay distance and power splitting ratio over certain limits significantly deteriorates the system performance, indicated by the decrease in the successful transmission probability.

Keywords: hybrid wireless and power line communication; wireless power transfer; energy harvesting; log-normal fading; opportunistic decode-and-forward and amplify-and-forward selection relaying; successful transmission probability

1. Introduction

The fifth-generation (5G) wireless communication is founded on the 4G/IMT-Advanced standards to serve the forecasted tens or even up to hundreds of billions of connected devices due to the continuous growth of state-of-the-art personal communication applications [1,2]. In the upcoming Internet of Things (IoT) era, it is predicted in [3–5] that by the year of 2030, there would be approximately 80 billion connected devices in a network and an individual can connect up to 20.5 billion devices simultaneously. Therefore, the expectation for the 5G communication has been that it can significantly improve the bandwidth, the data transmission rates, and the connectivity reliability and extend the network coverage while offering remarkable reductions in energy consumption and signal latency [3].

To enable long-lasting communication networks, several research studies have been conducted on self-sustaining simultaneous wireless information and power transfer (SWIPT) technology for energy harvesting (EH) from radio frequency (RF), firstly in [6] and ever since in [7–9]. There are two SWIPT protocols for the operation of receivers, namely time

switching-based relaying (TSR) and power splitting-based relaying (PSR), which were proposed in [10,11]. In TSR mode, the receiver can switch between information decoding (ID) and EH. On the other hand, PSR mode enables the receiver to partition the signal power into two parts dedicated to ID and EH. In [12], the authors studied the trade-off between the transmission outage probability (OP) and the ergodic capacity, respectively, versus the amount of energy harvested at the receiver in TSR and PSR scenarios. The energy efficiency (EE) of the SWIPT was studied in [13,14] and the physical-layer security aspect was investigated in [15–17].

Furthermore, to improve the EE, the spectrum efficiency (SE), the data transmission rates, and the throughput and coverage range, the cooperative relaying network has been investigated in [18–21]. Indeed, considerable diversity can be gained by exploiting several intermediate relays to aid the data transmission from the source node to the destination node [22]. Hence, two main cooperative relaying protocols, namely amplify-and-forward (AF) and decode-and-forward (DF), were investigated in [23]. Furthermore, a so-called ODF-AF selection relaying protocol that enables relays to adaptively switch between DF and AF considering their local signal-to-noise ratio (SNR) was proposed and investigated in [24–27]. It was proven in [28,29] that the ODF-AF scheme outperforms the standalone ODF and OAF schemes in terms of the outage performance of the system.

From relays' perspective, they can be operated in half-duplex (HD) and full-duplex (FD) modes. In the former, the relays are configured with one antenna utilizing the dedicated and orthogonal channels for re-transmitting data, while in the latter, with two antennas for data transmission within the same time slot and bandwidth. Furthermore, there is a hybrid HD-FD, which allows the opportunistic switch between the two aforementioned modes, and was proven to be able to deliver notably better performance, as studied in [30]. Wireless networks operating in FD mode can promisingly multiply the SE by two times and deliver significantly better network throughput in comparison with HD mode. Nevertheless, FD relays suffer self-interference because of the leaked signal between the two antennas [31], which inevitably degrades the system performance. Accordingly, in [32], the authors proposed different techniques to mitigate this loop interference for FD relaying networks along with their pros and cons.

As aforementioned, systems with higher diversity gain perform better thanks to the higher amount of independent fading signals that can be combined from multi-relay utilization [22,33], yet they face a higher risk of system degradation due to the higher level of inter-relay interference. To solve this, different relay selection (RS) schemes with their positive and negative effects on system performance were conducted in [34–37]. In particular, several different RS schemes for FD-AF cooperative networks were presented in detail in [34]. Paper [35] proposed a buffer-state-based RS scheme with the help of the Markov chain model. The authors in [36,37], respectively, studied the security improvement in DF cooperative relaying systems and the security-reliability trade-off of cognitive radio systems utilizing different RS schemes.

There are several studies about EH relaying SWIPT networks in the existing literature conducted over some prominent outdoor fading channel models, namely Nakagami-m, Rayleigh, and Rician. Nevertheless, for characterizing the shadowing effect of indoor scenarios owing to building walls, human body, and object mobilities, a so-called log-normal fading channel model was proven a better option [38–41]. The characteristics of common fading channel models along with their applications were investigated and compared in [42], and the appropriateness of the log-normal for indoor scenario modeling was proven in terms of small-scale fading and frequency of outage events. Additionally, there is paper [43], which studied the hybrid TSR-PSR protocol for EH networks, and paper [44], analyzing the performance of the two-hop AF relaying networks.

To efficiently promote the development of 5G networks for smart home and smart city applications, it is worth utilizing the existing power line communication (PLC) system that is present in every household. Indeed, PLC has regained the attention of the research community in recent years, being a well-founded medium for smart grids (SG) and IoT [45].

Besides the fact that PLC can notably reduce the installation cost, it can effectively establish communication with nodes that cannot be reached with RF due to the severe attenuation in the household setting. On the other hand, conventional PLC systems suffer from multipath fading effects and the in-line signal is degraded exponentially as the communication distance increases, which can be effectively tackled with the help of relay-aided networks [46]. Practically, because of the differences in the channel characteristics between the wireless and PLC networks, there is a need to implement dual-interface wireless–PLC relays as described in [47–49] for such hybrid wireless and PLC (HWP) networks to function. Research studies have proven that reliable signal transmission could be ensured even with a deterioration in quality on both links. Having deployed the dual-interface relays, it is then possible to apply all the aforementioned advantages of EH cooperative relaying networks on HWP, noting that, in the majority of studies, this has been achieved thanks to the help of time division multiple access (TDMA) schemes, as in [50–53].

With inspiration taken from the aforementioned studies, this manuscript focuses on the *STP* performance of the ODF-AF relaying selection in HD cooperative relaying networks given the indoor PLC condition making up the HWP, whose characteristics are modeled with log-normal fading channels. Subsequently, the main contributions of this manuscript are listed below:

- The *STP* for the direct link and ODF-AF relay-aided links of the dual-hop HD EH HWP over log-normal fading channels is analytically expressed.
- The *STP* and throughput performance of the ODF-AF selection relaying scheme in the HWP are analyzed and validated with Monte Carlo simulation results.

Moreover, it is worth noting the important notations utilized in this manuscript. Specifically, the probability density function (PDF) and the cumulative distribution function (CDF) of the log-normally distributed random variable (RV) X are, respectively, denoted as

$$F_X(z) = 1 - \mathcal{Q}\left(\frac{10\ln(10)^{-1}\ln(z)-2\omega_X}{2\Omega_X}\right) \text{ and } f_X(z) = \frac{10\ln(10)^{-1}}{z\sqrt{8\pi\Omega_X^2}} \exp\left(-\frac{(10\ln(10)^{-1}\ln(z)-2\omega_X)^2}{8\Omega_X^2}\right)$$

given the Gaussian \mathcal{Q} -function being $\mathcal{Q}(\cdot)$ with $\mathcal{Q}(x) = \int_x^\infty \frac{1}{\sqrt{2\pi}} \exp\left(-\frac{t^2}{2}\right) dt$. Moreover, there is \mathbb{E} , which represents the statistical mean operation.

Aside from the general Introduction in Section 1, Section 2 describes the system model with certain assumptions. In Section 3, the overall *STP* performance of the dual-hop HD EH HWP with ODF-AF relaying in EH-PSR protocol is derived. Accordingly, Section 4 reports the numerical results. Finally, Section 5 concludes the manuscript's findings and suggests possible future works. Furthermore, the abbreviations used in this manuscript are listed above the References section for ease of lookup.

2. System Model

In this study, a typical HWP system for indoor IoT is considered with dual-interface wireless–PLC relays integrated on all devices in the network, forming an Ad Hoc, as described in [47]. As mentioned earlier, PLC nodes will take the lead in establishing the communication among transceivers between several walls, and so do wireless nodes in case a lengthened power line notably downgrades the communication signal. As illustrated in Figure 1, a cooperative wireless relaying network is integrated into a PLC system for better communication between IoT devices, represented by a source (S), a destination (D), and a cluster (C) of K relays (R_i with $1 \leq i \leq K$). It is worth noting that PLC, IT, and PT, respectively, stand for the power line communication network, information transmission, and power transmission.

In the proposed HWP system, the received signals at the relaying nodes of both the interfaces can be described as follows.

$$\begin{bmatrix} y_p(t) \\ y_w(t) \end{bmatrix} = \begin{bmatrix} \sqrt{P} & 0 \\ 0 & \sqrt{P} \end{bmatrix} \begin{bmatrix} h_p & 0 \\ 0 & h_w \end{bmatrix} \begin{bmatrix} x(t) \\ x(t) \end{bmatrix} + \begin{bmatrix} n_p(t) \\ n_w(t) \end{bmatrix}, \quad (1)$$

where there are the transmitted symbol $x(t)$, channel gains from transmitting to receiving nodes over PLC and wireless channels, h_p and h_w , with noise, $n_p(t)$ and $n_w(t)$, and the transmission power P . In particular, for the HWP system, a module so-called signal decision processor (SDP) is deployed in the relaying node to evaluate and select the channel with the higher received SNR to forward the signal it received. Hence, the received SNR at the receiving node is expressed as follows.

$$\gamma = \max\left\{ Ph_p^2/n_p^2, Ph_w^2/n_w^2 \right\}. \quad (2)$$

For such a HWP system, it is obvious that there is a need to optimize both the PLC and the wireless channels. Within the scope of this study, it is assumed that the direct S–D link is under severe attenuation, and the communication is re-establishable neither by the PLC, due to lower received SNR, nor the direct wireless links, but solely via the cooperative relay-aided links. This assumption is equivalent to the wireless network in case there is either the coverage extension, where relays are utilized to establish the connection between significantly distant S–D [15,31], or when the direct S–D link is under a deep shadowing effect owing to the presence of the surrounding physical obstacles [54]. It is noteworthy that this setup has been utilized widely in the existing literature, with proven effectiveness in studying the cooperative networks and the potential diversity gain from such processes [15,31,54]. This setup is applicable even for cellular networks (LTE-Advanced), as in [55]. Furthermore, every terminal is aware of the channel state information (CSI) in advance and there is an ideal carrier and symbol synchronization. In addition, S is energized by a stable conventional power source P_S , and the i -th R is energized by the energy P_{R_i} from the EH module. In addition, n_j with $j \in \{r_k, d\}$ is defined as the additive white Gaussian noise (AWGN) with zero mean and variance N_0 at the i -th relay and D, respectively.

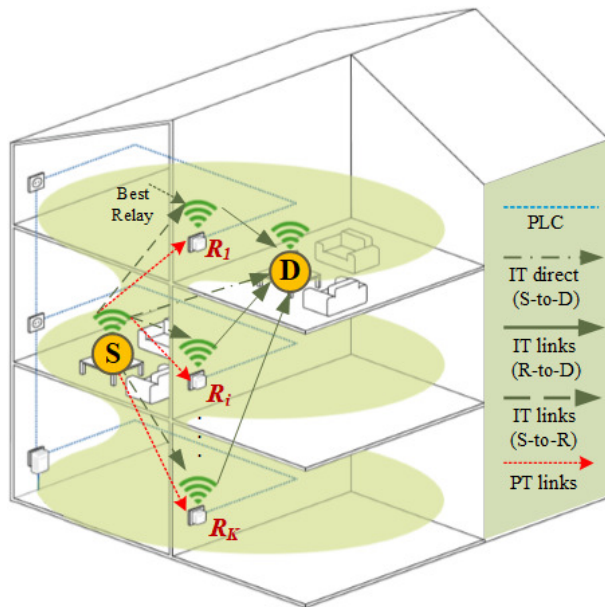


Figure 1. A typical HWP system with relaying nodes having both wireless and PLC interfaces. The relays scatter on different floors and rooms, and PLC relays are installed in electrical devices, which are connected with the power line.

It is assumed that the $S-R_i$ and R_i-D links are under the quasi-static block fading effect. This means that the channels remain constant over the block time, and they are independently and identically distributed (i.i.d.) following log-normal distribution from one block to another. As aforementioned, log-normal fading channels are utilized thanks to the appropriateness in modeling indoor scenarios with moving objects, furniture, and

several walls. The S– R_i , R_i –D and S–D links are with channel coefficients X , Y , and Z , respectively, and are correspondingly distant d_X , d_Y , and d_Z from each other. Similar to several studies dealing with log-normal fading channels [39], every communication node is equipped with one antenna, including the HD relays. Communication time is divided into slots given that, during a time slot interval, only a relay within C ($R_i \in C$) is selected for assisting the signal transmission from S.

Accordingly, the $|X|^2$, $|Y|^2$ and $|Z|^2$ are logically assumed as i.i.d. log-normal RVs, which are specified, respectively, with $LN(2\omega_X, 4\Omega_X^2)$, $LN(2\omega_Y, 4\Omega_Y^2)$, and $LN(2\omega_Z, 4\Omega_Z^2)$. It should be noted that both the ω_j and Ω_j^2 are in decibels (dB), and they respectively represent the mean and the standard deviation of $10 \log_{10}(j)$, $j \in \{X; Y; Z\}$.

First of all, a direct transmission protocol is considered, in which all time slots of a signal block are dedicated to the signal transmission of the direct S–D link. Accordingly, D receives the signal described by the base band-equivalent discrete-time model as follows:

$$y_Z = \sqrt{\frac{1}{d_Z^m}} Zs(t) + n_d(t), \quad (3)$$

where s indicates the narrow-band transmitted signal from S with zero mean, $\mathbb{E}[|s|^2] = P_S$, and m is the path loss exponent.

Consequently, the SNR for the direct S–D link obtained by utilizing the zero-mean, circularly symmetric, complex Gaussian inputs is expressed as

$$\gamma_Z = \Lambda \frac{|Z|^2}{d_Z^m}, \quad (4)$$

where $\Lambda = \frac{P_S}{N_0}$.

In addition, the instantaneous capacity of the S–D link is

$$C_{s,d} = W \log_2(1 + \gamma_Z), \quad (5)$$

where W stands for the frequency bandwidth.

In the direct transmission protocol, thanks to the CDF of the log-normally distributed RV $|Z|^2$, the STP can be formulated as

$$\begin{aligned} STP_{s,d} &= \Pr\{\gamma_Z \geq R_Z\} \\ &= 1 - \Pr\left\{|Z|^2 < \frac{R_Z}{\Lambda d_Z^{-m}}\right\} \\ &= \mathcal{Q}\left(\frac{10 \ln(10)^{-1} \ln\left(\frac{R_Z}{\Lambda d_Z^{-m}}\right) - 2\omega_Z}{2\Omega_Z}\right) \end{aligned} \quad (6)$$

where $R_Z = 2^{\frac{C_{th}}{W}} - 1$.

Furthermore, the STP is respectively formulated for the AF and DF protocols as follows

$$STP_{s,r,d}^{DF} = \Pr\left\{C_{s,r,d}^{DF} \geq C_{th}\right\}, \quad (7)$$

and

$$STP_{s,r,d}^{AF} = \Pr\left\{C_{s,r,d}^{AF} \geq C_{th}\right\}, \quad (8)$$

where $C_{s,r,d}^{DF} = \min\{C_r(\gamma_{ri}^{DF}), C_d(\gamma_{di}^{DF})\}$, and $C_{s,r,d}^{AF} = C_d(\gamma_{di}^{AF})$. C_r and C_d are, respectively, the instantaneous capacities at the i -th R and D, with the corresponding SNR being γ_{ri} and γ_{di} . C_{th} is a to-be-specified threshold value.

In the context of cooperative relaying networks where every relay utilizes the ODF-AF selection relaying protocol, the decoding state of R_i , $i \in 1, \dots, K$ is denoted as χ_i . If $\chi_i = 0$, then R_i utilizes the AF protocol for relaying the received signal. Otherwise, when $\chi_i = 1$, the DF protocol is utilized. Accordingly, the condition for the best relay k to be selected is

$$k = \arg \max_{i=1,2,\dots,N} \left\{ \chi_i \min \left\{ \gamma_{ri}^{DF}, \gamma_{di}^{DF} \right\} + (1 - \chi_i) \gamma_{di}^{AF} \right\}. \quad (9)$$

Accordingly, the STP of the ODF-AF selection relaying scheme can be obtained from

$$STP_k^{ODF-AF} = \left\{ \chi_k \Pr \left\{ \min \left\{ C_r(\gamma_{rk}^{DF}), C_d(\gamma_{dk}^{DF}) \right\} \geq C_{th} \right\} \right\} + (1 - \chi_k) \Pr \left\{ C_d(\gamma_{dk}^{AF}) \geq C_{th} \right\}. \quad (10)$$

Remark 1. *STP is utilized to evaluate the system performance of the proposed relay-aided cooperative protocol. It is defined as the probability of a receiver succeeding in receiving packets from its corresponding transmitter within a time slot interval. Specifically, in this study, the transmission time is slotted, in which S, R, and D take turns to send their packets when each slot begins. Specifically, when S attempts to send some of its packets, if the instantaneous capacity is greater than a pre-specified threshold value, an acknowledgement signal (ACK) will be sent to S indicating that R has succeeded in receiving the packets. These packets are then removed from the queue at S. Otherwise, they remain on top of the queue. From R, they are eventually transmitted in a similar manner to D to accomplish one transmission circle. It is noteworthy that the STP formulation can be extended to multi-hop networks, given that every slot of the networks must be considered, instead of solely two slots, as in this dual-hop case.*

For the PSR protocol, the block time T is halved, with one half utilized for the signal transmission of the S–R link and the other for the R–D link. Within the first half interval, a portion of the signal power that R receives, being δP_S , is allocated for the EH module given the PS factor δ and $0 \leq \delta \leq 1$. The rest of the signal power, being $(1 - \delta)P_S$, is utilized for signal transmission. In case $\delta = 1$, the system operates in full EH mode, and $\delta = 0$ in full ID mode.

Thus, within the first time slot, the EH module receives the input signal of

$$\sqrt{\delta}y_r(t) = \sqrt{\delta} \sqrt{\frac{1}{d_X^m}} Xs(t) + n_r(t). \quad (11)$$

Moreover, the base-band signal at the information receiver, being $\sqrt{1 - \delta}\gamma_r(t)$, is expressed for both AF and DF as

$$\sqrt{1 - \delta}y_r(t) = \sqrt{(1 - \delta)} \sqrt{\frac{1}{d_X^m}} Xs(t) + n_r(t). \quad (12)$$

In this protocol, R only harvests, within each block interval, enough energy required to perform its relaying task [56] (Sec. III-B). Thus, when each time block ends, there is no energy remaining in R. This harvested energy during the first phase is obtained by

$$E_H = \frac{\eta \delta P_S |X|^2 T}{2 d_X^m}, \quad (13)$$

where $0 \leq \eta \leq 1$ is the EH efficiency characterized by the property of the circuitry.

During the $T/2$ interval, all of the harvested energy is consumed by R to re-transmit the message from S to D with power P_R . Hence, the amount of harvested energy at the instantaneous $T/2$ time is

$$E_H = P_R \frac{T}{2}. \quad (14)$$

As (13) is equal to (14), δ^* can be obtained as

$$\delta^* = \frac{P_R}{\eta \delta P_S} \frac{d_X^m}{|X|^2}. \quad (15)$$

Accordingly, the relay's transmitting power, as in [6,18], is given by

$$P_R = \frac{\eta \delta P_S |X|^2}{d_X^m}. \quad (16)$$

Remark 2. It is noteworthy that the direct link and relay links are available for information transmission in the proposed relay-aided cooperative HWP system. One R with a sufficient harvested energy amount among ks is selected to establish the relay-aided link to substitute the deep faded direct link. Additionally, it is proven in [40] that the application of RS schemes in systems powered by an EH module can help to attain the maximum diversity gain amounting to the number of operated R nodes over the i.i.d. log-normal fading channel.

3. Performance Analysis

In this section, the STP of the HD cooperative relaying HWP system over log-normal fading channels is investigated for the DF and AF protocols.

3.1. Opportunistic Decode-and-Forward (ODF) Relaying Scheme

Within the second time slot, as the name suggests, the signal from (16) is decoded, re-modulated, and then forwarded utilizing the harvested energy from (13). Thereby, in the HD-DF HWP system, at D, the received signal can be obtained from

$$y_d(t) = \sqrt{\frac{1}{d_Y^m}} Y \bar{s}(t) + n_d(t), \quad (17)$$

where \bar{s} is the narrow-band transmitted signal at i -th R with zero mean and $\mathbb{E}[|\bar{s}|^2] = P_R$.

Combining (12), (16) and (17), one can express the SNRs at the i -th R and D, respectively, as

$$\gamma_{ri}^{DF} = \frac{(1 - \delta)\Lambda}{d_X^m} |X|^2, \quad (18)$$

and

$$\gamma_{di}^{DF} = \frac{\eta \delta \Lambda}{d_X^m d_Y^m} |X|^2 |Y|^2. \quad (19)$$

In the HD-DF-PSR HWP system, the instantaneous capacity of the first and second links can be obtained from

$$C_j = \frac{1}{2} W \log_2 \left(1 + \gamma_{ji}^{DF} \right), \quad (20)$$

where $j \in \{r, d\}$, and the HD relaying factor $\frac{1}{2}$.

Theorem 1. The STP of the HD-DF-PSR HWP system is formulated as

$$\begin{aligned} ST\mathcal{P}_{s,r,d}^{DF} = & \mathcal{Q}\left(\frac{10 \ln(10)^{-1} \ln(a_1) - 2\omega_X}{2\Omega_X}\right) \\ & - \frac{10 \ln(10)^{-1}}{\sqrt{8\pi\Omega_X^2}} \int_{a_1}^{\infty} \frac{1}{x} \exp\left(-\frac{(10 \ln(10)^{-1} \ln(x) - 2\omega_X)^2}{8\Omega_X^2}\right) \\ & \times \left(1 - \mathcal{Q}\left(\frac{10 \ln(10)^{-1} \ln(a_2 x^{-1}) - 2\omega_Y}{2\Omega_Y}\right)\right) dx, \end{aligned} \quad (21)$$

where $R_{th} = 2^{2C_{th}/W} - 1$, $a_1 = d_X^m R_{th} / (1 - \delta)\Lambda$, and $a_2 = d_X^m d_Y^m R_{th} / \eta\delta\Lambda$.

Proof. With regard to (7), the STP is re-organized as

$$\begin{aligned} ST\mathcal{P}_{s,r,d}^{DF} = & \Pr\left\{\min\left\{C_r(\gamma_{ri}^{DF}), C_d(\gamma_{di}^{DF})\right\} \geq C_{th}\right\} \\ = & \Pr\left\{C_r(\gamma_{ri}^{DF}) \geq C_{th}, C_d(\gamma_{di}^{DF}) \geq C_{th}\right\} \\ = & \underbrace{\Pr\left\{C_r(\gamma_{ri}^{DF}) \geq C_{th}\right\}}_{ST\mathcal{P}_1^{DF}} \cap \underbrace{\Pr\left\{C_d(\gamma_{di}^{DF}) < C_{th}\right\}}_{ST\mathcal{P}_2^{DF}}. \end{aligned} \quad (22)$$

To calculate the STP in the HD-DF-PSR HWP system, two probability calculations are required. From (18) and (20), the first probability in (22) can be rewritten in detail as

$$\begin{aligned} ST\mathcal{P}_1^{DF} = & \Pr\left\{\frac{1}{2} \log_2\left(1 + \frac{(1 - \delta)\Lambda|X|^2}{d_X^m}\right) \geq C_{th}\right\} \\ = & \Pr\left\{|X|^2 \geq R_{th} \frac{d_X^m}{(1 - \delta)\Lambda}\right\} \\ = & 1 - F_X\{a_1\} \\ = & \mathcal{Q}\left(\frac{10 \ln(10)^{-1} \ln(a_1) - 2\omega_X}{2\Omega_X}\right) \end{aligned} \quad (23)$$

where there are the CDF of the log-normally distributed RV $X = |X|^2$, $R_{th} = 2^{2C_{th}} - 1$, and $a_1 = \frac{d_X^m R_{th}}{(1 - \delta)\Lambda}$.

Likewise, (18)–(20) are utilized for calculating the second probability in (22) as

$$\begin{aligned} ST\mathcal{P}_2^{DF} = & \Pr\left\{X \geq a_1, \frac{\eta\delta\Lambda XY}{d_X^m d_Y^m} < R_{th}\right\} \\ = & \Pr\left\{X \geq a_1, Y < \frac{a_2}{X}\right\} \end{aligned} \quad (24)$$

where $Y = |Y|^2$, and $a_2 = \frac{d_X^m d_Y^m R_{th}}{\eta\delta\Lambda}$.

Then, thanks to the PDF and CDF of the log-normally distributed RVs X and Y , the $ST\mathcal{P}_2^{DF}$ can be rewritten as

$$\begin{aligned} ST\mathcal{P}_2^{DF} &= \int_{a_1}^{\infty} f_X(z) F_Y\left(\frac{a_2}{z}\right) dz \\ &= \int_{a_1}^{\infty} \frac{10 \ln(10)^{-1}}{z \sqrt{8\pi\Omega_X^2}} \exp\left(-\frac{(10 \ln(10)^{-1} \ln(z) - 2\omega_X)^2}{8\Omega_X^2}\right) \\ &\quad \times \left(1 - \mathcal{Q}\left(\frac{10 \ln(10)^{-1} \ln(a_2 z^{-1}) - 2\omega_Y}{2\Omega_Y}\right)\right) dz. \end{aligned} \quad (25)$$

Eventually, (24) and (25) are substituted into (23) to obtain the $ST\mathcal{P}$ of the HD-DF-PSR HWP system over log-normal fading channels as given in (21). The proof ends here. \square

3.2. Opportunistic Amplify-and-Forward (OAF) Relaying Scheme

For the HD-AF-PSR HWP system, with the harvested energy in (13), R amplifies and forwards the signal from S to D. Thereby, the R's transmitted signal can be obtained as follows:

$$x_r(t) = \sqrt{(1-\delta)} \sqrt{\frac{1}{d_X^m} \mathcal{G} X s(t) + \mathcal{G} n_r(t)}, \quad (26)$$

where $\mathbb{E}[|s|^2] = P_S$, and the relay gain of the HD-AF-PSR HWP system is obtained from

$$\mathcal{G} = \sqrt{\frac{P_R}{\left(\frac{(1-\delta)P_S}{d_X^m} X + N_0\right)}} \quad (27)$$

Accordingly, the signal that D receives is

$$\begin{aligned} y_d(t) &= \sqrt{\frac{1}{d_Y^m}} Y x_r(t) + n_d(t) \\ &= \sqrt{(1-\delta)} \sqrt{\frac{1}{d_X^m d_Y^m}} \mathcal{G} X Y s(t) + \sqrt{\frac{1}{d_Y^m}} \mathcal{G} Y n_r(t) + n_d(t). \end{aligned} \quad (28)$$

Then, (16) and (27) are substituted into (28) and then manipulated to obtain the SNR at D as follows:

$$\gamma_{di}^{AF} = \frac{\eta\delta(1-\delta)\Lambda XY}{\eta\delta d_X^m Y + \eta\delta(1-\delta)d_X^m Y + (1-\delta)d_X^m d_Y^m}. \quad (29)$$

In the HD-AF-PSR HWP system, the system's instantaneous capacity is expressed as

$$C_d = \frac{1}{2} \log_2 \left(1 + \gamma_{di}^{AF}\right). \quad (30)$$

Theorem 2. In the aforementioned context, the $ST\mathcal{P}$ in the HD-AF-PSR HWP system can be formulated as

$$\begin{aligned} ST\mathcal{P}_{s,r,d}^{AF}(R_{th}) &= \frac{10 \ln(10)^{-1}}{\sqrt{8\pi\Omega_X^2}} \int_{R_{th}(b_2+b_3)}^{\infty} \frac{1}{z} \mathcal{Q}\left(\frac{10 \ln(10)^{-1} \ln(\Gamma) - 2\omega_Y}{2\Omega_Y}\right) \\ &\quad \times \exp\left(-\frac{(10 \ln(10)^{-1} \ln(z) - 2\omega_X - 10 \ln(10)^{-1} \ln(b_1))^2}{8\Omega_X^2}\right) dz, \end{aligned} \quad (31)$$

where $b_1 = \eta\delta(1-\delta)\Lambda$, $b_2 = \eta\delta d_X^m$, $b_3 = \eta\delta(1-\delta)d_X^m$, $b_4 = (1-\delta)d_X^m d_Y^m$, and $\Gamma = \frac{R_{th}b_4}{z-R_{th}(b_2+b_3)}$.

Proof. For more easily deriving the $ST\mathcal{P}$ of the proposed HD-OAF-PSR HWP system, (29) is rewritten as

$$\gamma_d^{AF} = \frac{b_1XY}{b_2Y + b_3Y + b_4}, \quad (32)$$

with b_1 , b_2 , and b_3 given in (31).

Then, (32) is substituted to (8) to obtain

$$\begin{aligned} ST\mathcal{P}_{s,r,d}^{AF} &= \Pr\left\{\frac{b_1XY}{b_2Y + b_3Y + b_4} \geq R_{th}\right\} \\ &= 1 - \Pr\left\{Y < \frac{R_{th}b_4}{b_1X - R_{th}(b_2 + b_3)}\right\}. \end{aligned} \quad (33)$$

As Y is positive, the probability $\mathcal{P} = \Pr\left\{Y < \frac{R_{th}b_4}{b_1X - R_{th}(b_2 + b_3)}\right\}$ can be decomposed to

$$\mathcal{P} = \begin{cases} \Pr\left\{Y \geq \frac{R_{th}b_4}{b_1X - R_{th}(b_2 + b_3)}\right\} = 1, & X > \frac{R_{th}(b_2 + b_3)}{b_1} \\ \Pr\left\{Y < \frac{R_{th}b_4}{b_1X - R_{th}(b_2 + b_3)}\right\}, & X < \frac{R_{th}(b_2 + b_3)}{b_1} \end{cases} \quad (34)$$

The $ST\mathcal{P}$ in (33) can be obtained from

$$ST\mathcal{P}_{s,r,d}^{AF} = 1 - \left[\int_0^{z=\frac{R_{th}(b_2+b_3)}{b_1}} f_X(z) dz + \int_{z=\frac{R_{th}(b_2+b_3)}{b_1}}^{\infty} f_X(z) \Pr\left\{Y < \frac{R_{th}b_4}{b_1X - R_{th}(b_2 + b_3)}\right\} dz \right], \quad (35)$$

where $f_X(\cdot)$ and $F_Y(\cdot)$ represent, respectively, the PDF and the CDF of the log-normally distributed RVs X and Y . The two functions are given below:

$$f_X(z) = \frac{10 \ln(10)^{-1}}{z \sqrt{8\pi\Omega_X^2}} \exp\left(-\frac{(10 \ln(10)^{-1} \ln(z) - 2\omega_X - 10 \ln(10)^{-1} \ln(b_1))^2}{8\Omega_X^2}\right), \quad (36)$$

and

$$F_Y\left(\frac{R_{th}b_4}{z - R_{th}(b_2 + b_3)}\right) = 1 - Q\left(\frac{10 \ln(10)^{-1} \ln\left(\frac{R_{th}b_4}{z - R_{th}(b_2 + b_3)}\right) - 2\omega_Y}{2\Omega_Y}\right). \quad (37)$$

Consequently, (36) and (37) are substituted into (35) to obtain the $ST\mathcal{P}$ of the DF-AF-PSR system as in (30). \square

3.3. Opportunistic Decode-and-Forward and Amplify-and-Forward (ODF-AF) Relaying Scheme

Utilizing Theorem 1 and 2, the overall successful event is established with the help of the Selection Combining (SC) method, which combines the $ST\mathcal{P}$ of the direct link and the ODF-AF relay-aided links to apply for the HWP system. It is noteworthy that the diversity order analysis is not affected with SC. Subsequently, from the condition of $\{\text{good direct link}\} \cup_k \{\text{good } k\text{-th ODF-AF relay-aided link}\}$, the below expression can be obtained:

$$\begin{aligned} ST\mathcal{P}^{sc} &= ST\mathcal{P}_{s,d} \times \prod_{k=1}^K \left\{ (1 - \chi_k) ST\mathcal{P}_{s,r,d}^{AF} + \chi_k ST\mathcal{P}_{s,r,d}^{DF} \right\} \\ &= \mathcal{A}_0 \times \prod_{k=1}^K \left((1 - \chi_k) \left(\int_{\gamma_1}^{\infty} A_1(x) \times A_2(x) \right) + \chi_k \left(A_3 - \int_{\gamma_2}^{\infty} A_4(x) \right) \right)', \end{aligned} \quad (38)$$

where

$$\mathcal{A}_0 = \mathcal{Q}\left(\frac{5}{\Omega_Z \ln(10)} \ln\left(\frac{R_Z}{\Lambda d_Z^{-m}}\right) - \frac{\omega_Z}{\Omega_Z}\right), \quad (39)$$

$$\mathcal{A}_1(x) = \frac{1}{x} \mathcal{Q}\left(\frac{5}{\Omega_Y \ln(10)} \left(\frac{(1-\delta)d_X^m d_Y^m R_{th}}{x - \eta \delta d_X^m R_{th}(2-\delta)}\right) - \frac{\omega_Y}{\Omega_Y}\right), \quad (40)$$

$$\mathcal{A}_2(x) = \frac{5}{\ln(10)\sqrt{2\pi\Omega_X^2}} \exp\left(-\frac{\left(10\ln(10)^{-1}\ln(x) - 2\omega_X - 10\ln(10)^{-1}\ln(\eta\delta(1-\delta)\Lambda)\right)^2}{8\Omega_X^2}\right) \quad (41)$$

$$\mathcal{A}_3 = \mathcal{Q}\left(\frac{5}{\Omega_X \ln(10)} \ln\left(\frac{d_X^m R_{th}}{(1-\delta)\Lambda}\right) - \frac{\omega_X}{\Omega_X}\right), \quad (42)$$

$$\begin{aligned} \mathcal{A}_4(x) = & \frac{1}{x} \frac{5}{\ln(10)\sqrt{2\pi\Omega_X^2}} \exp\left(-\frac{\left(10\ln(10)^{-1}\ln(x) - 2\omega_X\right)^2}{8\Omega_X^2}\right) \\ & \times \left(1 - \mathcal{Q}\left(\frac{5}{\Omega_Y \ln(10)} \ln\left(\frac{d_X^m d_Y^m R_{th}}{\eta\delta\Lambda} \frac{1}{x}\right) - \frac{\omega_Y}{\Omega_Y}\right)\right) dx, \end{aligned} \quad (43)$$

and $\varphi_1 = \eta\delta d_X^m (2-\delta) R_{th}$, $\varphi_2 = \frac{d_X^m R_{th}}{(1-\delta)\Lambda}$.

3.4. Throughput Performance

In this subsection, the throughput, τ , of delay-constrained HWP systems is determined. It is given that S transmits data with a constant rate of R_{th} (bps/Hz) and the S–D effective communication time over the time block is $T/2$ over T (s). The HWP systems are subject to outage events owing to the log-normal fading effect on the wireless channels. Hence, the average throughput in the delay-constrained scenario is formulated in [29] as follows:

$$\tau^{sc} = \frac{T/2}{T} (1 - \mathcal{OP}^{sc}) R_{th}, \quad (44)$$

where, thanks to Theorems 1 and 2, the outage probability, \mathcal{OP}^{sc} , in the multi-relay scenario is established utilizing (38) as $\mathcal{OP}^{sc} = (1 - ST\mathcal{P}_{s,d}) \times \left[(1 - \chi_k)(1 - ST\mathcal{P}_{s,r,d}^{AF}) + \chi_k(1 - ST\mathcal{P}_{s,r,d}^{DF})\right]^K$.

4. Numerical Results and Discussion

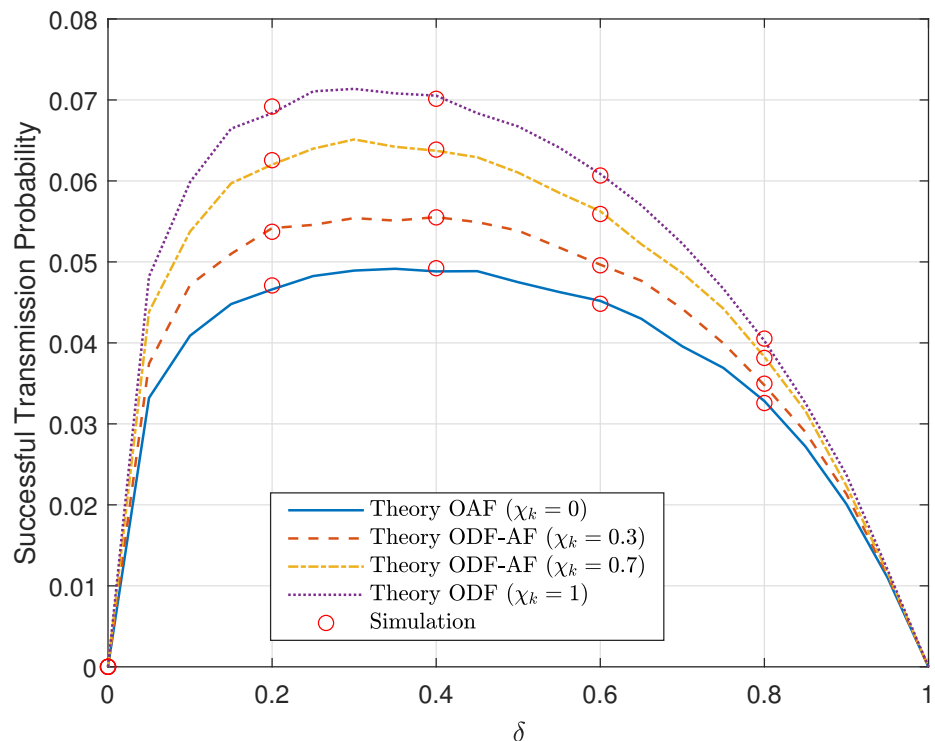
This section presents the Monte Carlo simulation results from Matlab for the above analytical expressions. The parameters used for the simulation are listed in Table 1 below. With the exception of Figure 7, in all the figures, the number of relays is fixed at $K = 3$. Moreover, the utilized $ST\mathcal{P}$ henceforth stands for the $ST\mathcal{P}$ of the HWP system where the direct and relay-aided links are combined.

Figure 2 plots the overall analytical and simulated $ST\mathcal{P}$ of the ODF-AF HWP systems concerning the EH PS ratio, δ , with four different decoding-state probabilities at the best-selected R, χ_k . The power transmission at S is $P_S = -10$ (dB). The simulated results agree well with the analytical ones, proving the feasibility of the above derivations. As aforementioned, at $\chi_k = 0$, the best R fully utilizes the ODF selection relaying protocol to decode and forward the message from S via direct link. At $\chi_k = 1$, the OAF one is utilized and the best relay performs its task accordingly. Aside from the two extreme cases, in the two other ODF-AF protocol cases, $\chi_k = 0.3$ and 0.7 are plotted as well. It can be observed that all the curves rise linearly and sharply as δ goes from 0 to approximately 0.05. Then, the $ST\mathcal{P}$ values exponentially grow and peak with a lower pace as δ reaches 0.2 and then 0.4. Henceforth, all the $ST\mathcal{P}$ curves converge exponentially to 0 as δ approaches 1.

Table 1. Simulation parameters.

Primary Parameters	Description	Values
W	frequency bandwidth	5 (W)
R_0	transmission rate threshold	1 (bps/Hz)
P_S	traditional stabilized power source	-10 (dB)
N_0	overall AWGNs	1
η	energy harvesting efficiency	1
δ	power splitting fraction	0.2
m	path-loss	2.7
d_X	S to R distance	1 (m)
d_Y	R to D distance	1 (m)
d_Z	S to D distance	2 (m)
Ω_X	S to R channel mean, log-normally distributed	4 (dB)
Ω_Y	R to D channel mean, log-normally distributed	4 (dB)
Ω_Z	S to D channel mean, log-normally distributed	4 (dB)
ω_X	S to R channel variance, log-normally distributed	3 (dB)
ω_Y	R to D channel variance, log-normally distributed	3 (dB)
ω_Z	S to D channel variance, log-normally distributed	3 (dB)
K	Number of relays	3

It is noteworthy in Figure 3 that as $P_S = 1$ (dB), the STP has significantly improved and the curves become flatter. The STP remains peaked as $\chi_k = 0.4$ and has remarkably raised from 0.07 to approximately 0.67. This means that up to 40% of the power transmission $P_S = 1$ (dB) can be allocated to the EH module to obtain the optimized performance. Indeed, the power transmission values used in Figures 2 and 3 are rather small, -10 (dB) and 1 (dB). Given that the input power can be set to a higher value, the STP could accordingly raise to its maximum.

**Figure 2.** STP versus the PS ratio, δ , when $P_S = -10$ (dB).

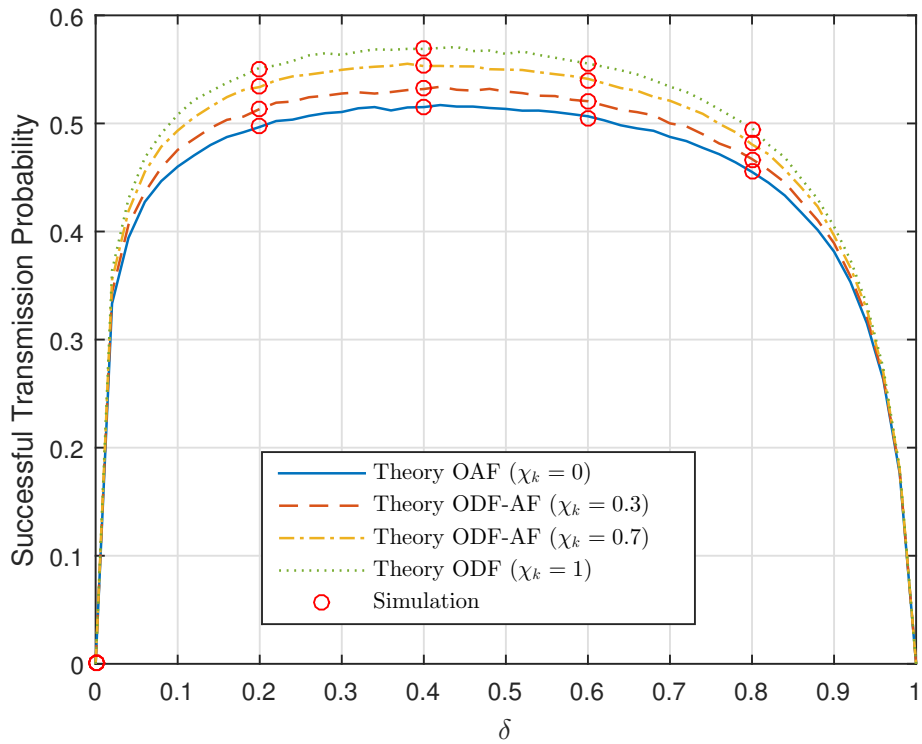


Figure 3. STP versus the PS ratio, δ , when $P_S = 1$ (dB).

The fact that the STP curves drastically rise from and fall to 0 as δ , respectively, starts at 0 and approaches 1 is because the harvested energy in these two cases is either too small or undesirably too large that no resource is left for data transmission. In particular, the OAF delivers the lowest STP . Additionally, the probability to utilize the ODF becomes greater as χ_k value changes from 0.3 to 0.7 and finally 1. Subsequently, the higher the STP curve becomes, leading to better system performance. Optimizing the δ value is of importance for system performance and, thankfully, this task is realized in a thorough manner utilizing solely theory and Equation (15). Lastly, it is worth stating that the system performance can further be improved by unequally allocating the channels concerning the relative channel distributions.

Figure 4 presents the STP of the ODF-AF selection relaying scheme versus the SNR in the HWP system. The rise in the SNR logically results in better STP . The STP exponential curves rise rapidly as SNR approaches 10 (dB) and slowly converge to 1 as SNR grows further. As previously concluded, the ODF scheme performs better than the OAF one. This means that in the EH-PSR scenario, when SNR becomes larger, it is more beneficial to utilize the power to perform the ID task. Additionally, without spectrum sharing, the ODF-AF scheme performs better as the probability to utilize the ODF scheme increases.

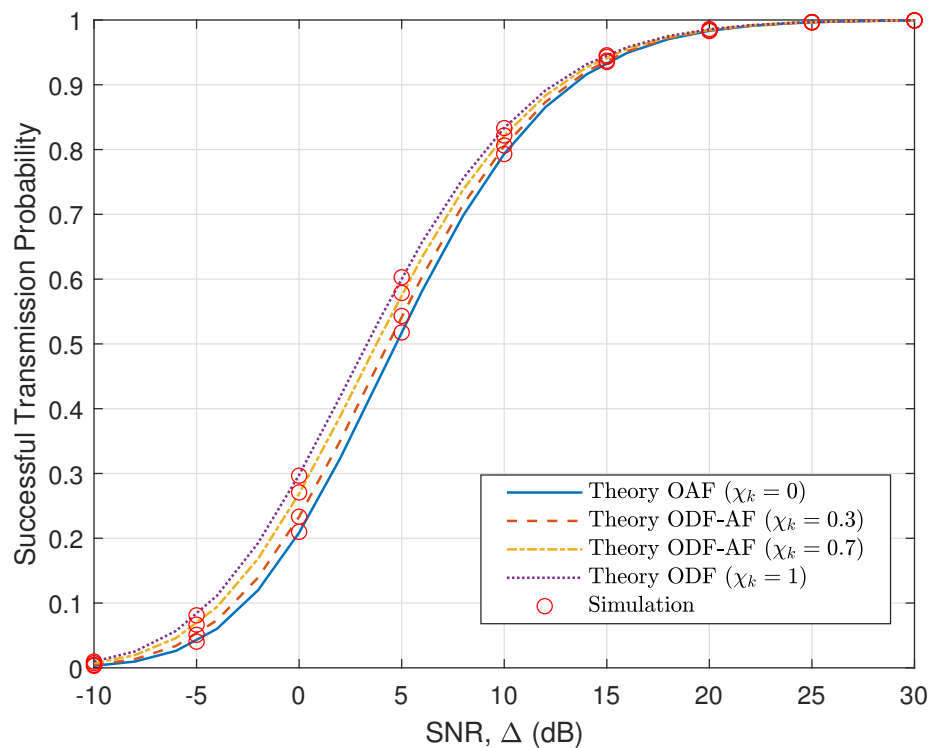


Figure 4. STP versus SNR.

Figure 5 illustrates the STP of the ODF-AF-PSR scheme versus SNR in the HWP system, with two distance sets being Case 1: $d_X = d_Y = 1$ (m); $d_Z = d_X + d_Y = 2$ (m), and Case 2: $d_X = d_Y = 2$ (m); $d_Z = d_X + d_Y = 4$ (m). The trend of the curves in the two cases is the same as in Figure 4. It is obvious that Case 1 performs remarkably better than Case 2 owing to the shorter distances between terminals. This is because as the distances increase, the EH power and the signal strength that R receives are reduced significantly due to the path loss increase. Accordingly, the signal strength that D receives is also more attenuated, leading to the STP decrease. Figure 6 reveals the STP versus the SNR of the HWP system concerning two different cases of threshold values $R_0 = 1$ and 2 (bps/Hz). The OAF is represented with continuous lines, ODF-AF with dashed lines, and ODF with dash-dotted lines. As SNR increases from -10 (dB) to 0 (dB) for $R_0 = 2$, or 5 (dB) for $R_0 = 1$, the throughput rises exponentially, with ODF always being the highest. Nevertheless, after reaching their peaks, there is no difference in throughput as these curves remain at the same value regardless of the increase in the SNR. It is worth noting that the greater the opportunity to choose the ODF protocol, the higher the starting level of throughput, at SNR = -10 (dB).

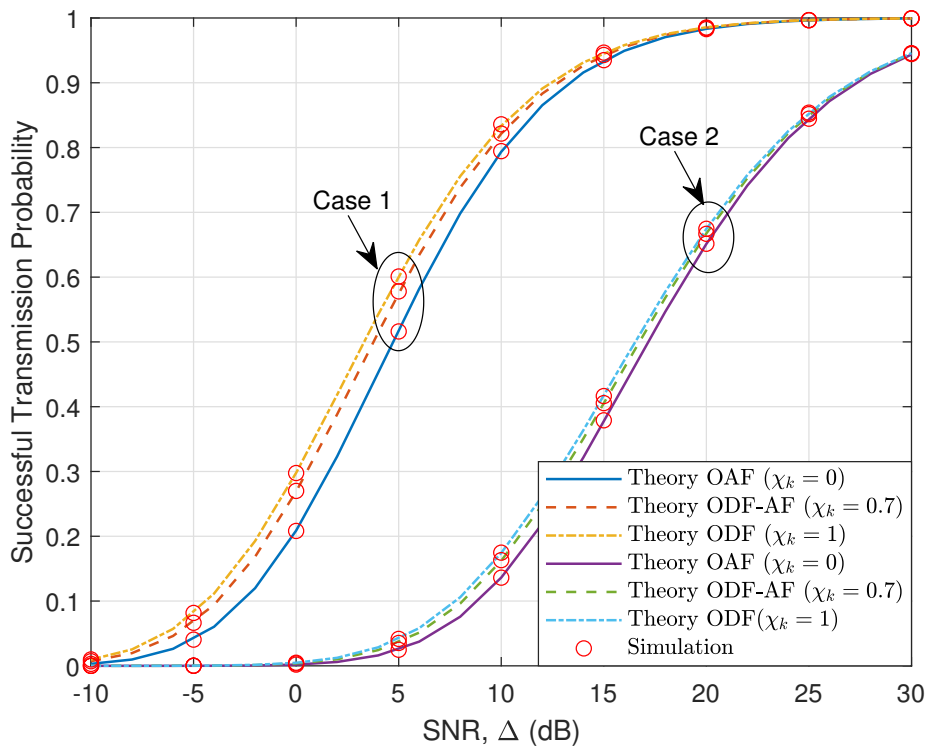


Figure 5. STP versus SNR in two different modes: Case 1 and Case 2.

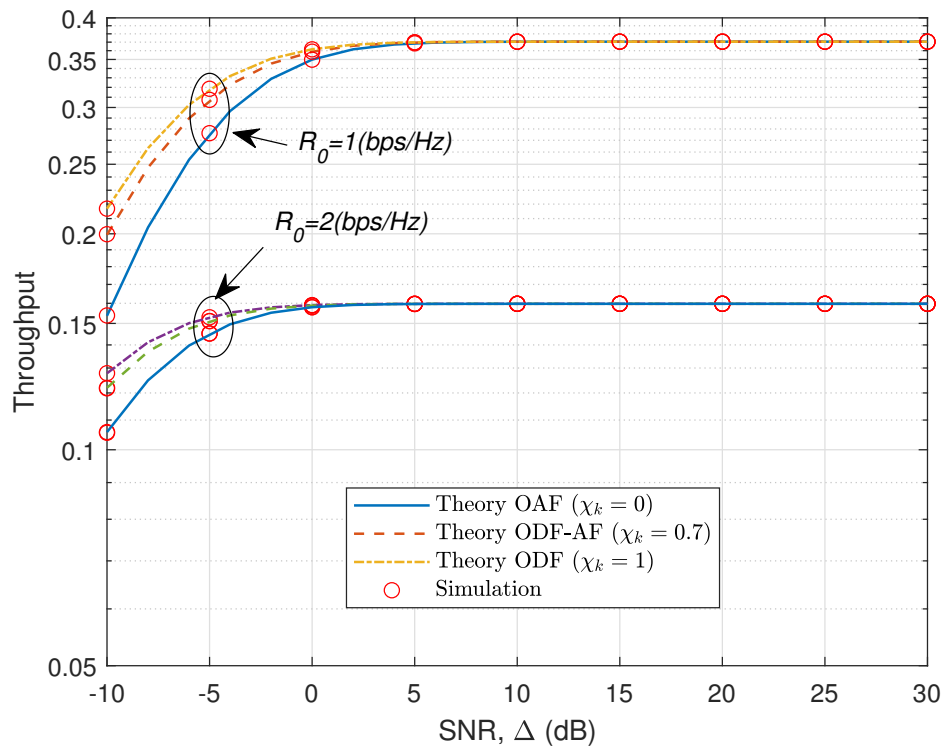


Figure 6. STP versus SNR with two different threshold values $R_0 = 1$ and $R_0 = 2$ (bps/Hz).

Figure 7 depicts the throughput analysis of the ODF-AF-PSR scheme at D versus the number of relays in the HWP system, K , with the power transmission of S being $P_S = -10$ (dB). Similar to what has been drawn previously, the ODF scheme has notably

better performance than the OAF one. As there are more relays, the coding gain rises in association with the data transmission rates, leading to the throughput increase.

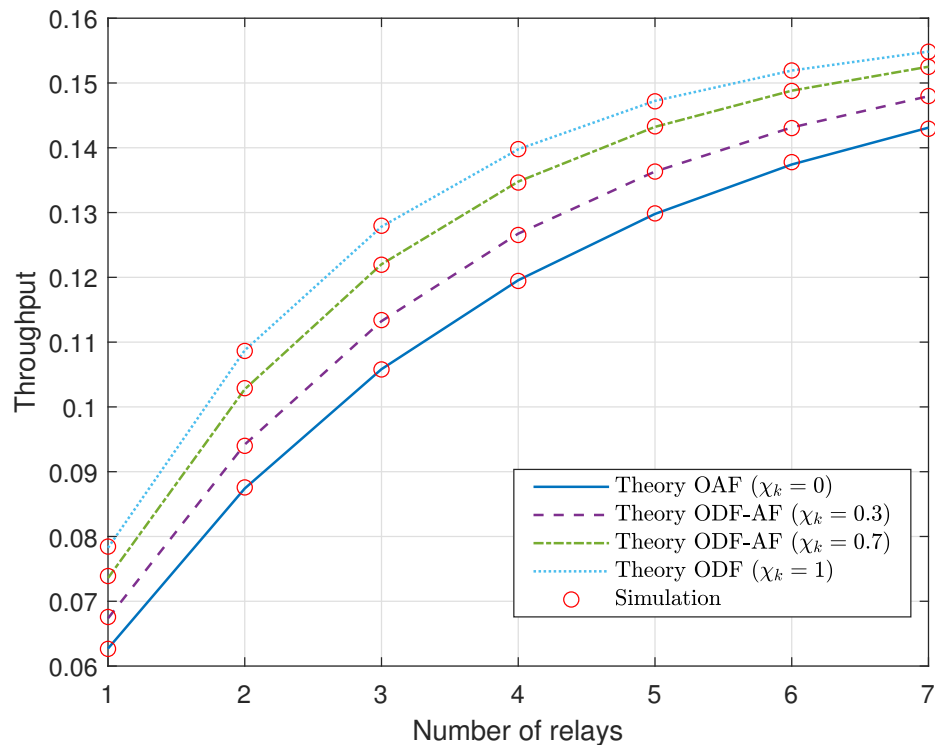


Figure 7. The throughput at D versus the number of R, K.

Figure 8 plots the STP versus different values of d_X of the HWP system given that $d_Z = 10$ and $d_Y = d_Z - d_X$. It can be observed that the ODF theoretically performs better than OAF and ODF-AF no matter the location of R within the d_Z range. Nonetheless, starting from the highest at (0.69), all the STP curves converge rapidly to (0.08) floor as R moves further to the midpoint of the S-D range. This is because as R moves towards the midway, it spends more time on EH; thus, the transmission time is shortened.

By utilizing the log-normal fading channels, the RF communication in an indoor scenario, through walls and with the presence of furniture and moving objects, was modeled in this study. The obtained simulation results show the system performance in terms of the STP of the proposed scheme in the HWP setting. Additionally, readers can make use of the simulation results to optimize the data rates without the need for additional bandwidth or power.

Lastly, what can be generally concluded from all the figures is that there is good agreement between the simulated and the analytical results. Thereby, the expressions derived herein can be utilized for future works.

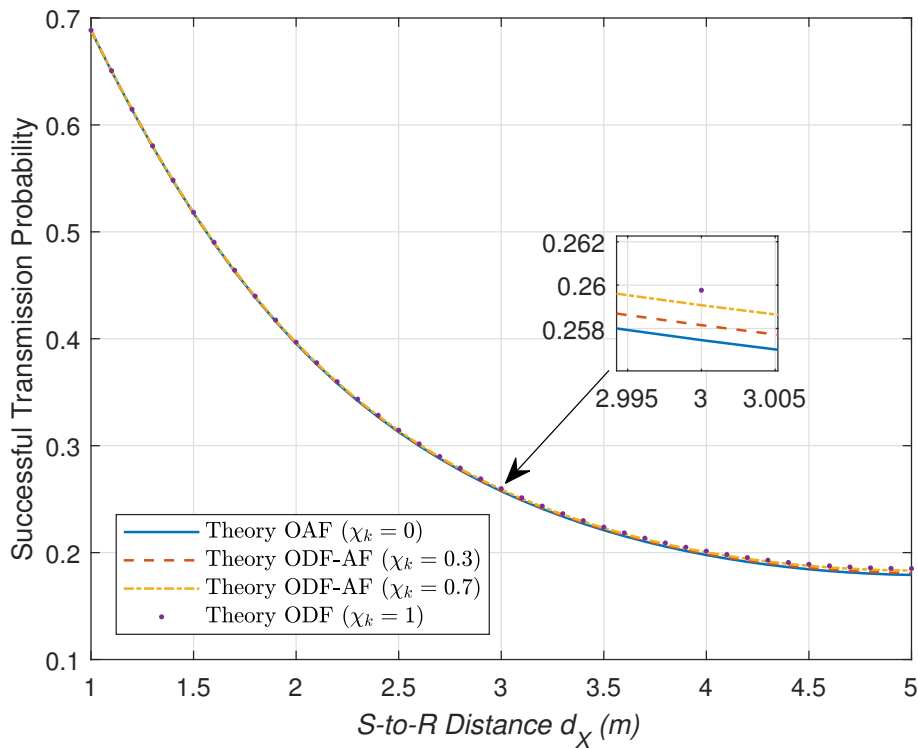


Figure 8. STP versus different S–R distance values, d_X , on condition that $d_Z = 10$ (m), $d_Y = d_Z - d_X$.

5. Conclusions

To summarize, this manuscript aims at analyzing the behaviors of the opportunistic decode-and-forward and amplify-and-forward relay selection scheme in an energy harvesting power splitting-based relaying hybrid wireless and power line communication system over log-normal fading channels for indoor IoT networks. In particular, the issue of how to select an optimal relay for maximizing the signal-to-noise ratio that the destination receives is studied in terms of the successful transmission probability. Analytical expressions are derived and proven with relatively high accuracy thanks to Monte Carlo simulation results. The opportunistic decode-and-forward scheme is capable of delivering considerably better successful transmission probability in comparison with the opportunistic amplify-and-forward one. Additionally, the simulation results reveal that as the power splitting ratio and the source-to-relay distance increase, the system performance is subsequently degraded. The workflow presented in this manuscript can be followed by network designers who are interested in hybrid wireless and power line communication systems, given the assumptions and accuracy of the formulations. Lastly, the focus of future study will be the optimal hybrid decode-and-forward and amplify-and-forward protocol in cooperative relaying hybrid wireless and power line communication systems. Solving the newly emerging problems in combining and optimizing the two mature technologies as studied herein is promising as it brings about vast benefits, especially cost efficiency, for 5G smart home and smart city applications.

Author Contributions: Conceptualization, H.-S.N., M.V., methodology, H.T.V., H.-P.V., H.-S.N., experimental analysis and set-up, H.T.V., D.H.L., Q.-N.V., J.J.; writing—original draft preparation, H.-P.V., H.T.V., J.J., D.H.L. All authors have read and agreed to the published version of the manuscript.

Funding: The research leading to these results was supported by the Czech Ministry of Education, Youth and Sports under project reg. no. SP2021/25 and also partially by the project “e-Infrastructure CZ” reg. no. LM2018140. Thanks to Saigon International University (SIU) for supporting this project.

Institutional Review Board Statement: Not applicable.

Informed Consent Statement: Not applicable.

Data Availability Statement: Our study does not report any data.

Conflicts of Interest: The authors declare that they have no conflicts of interest.

Abbreviations

Below are the abbreviations that are used in this manuscript:

5G	Fifth generation of cellular networks
EH	Energy harvesting
RF	Radio frequency
SWIPT	Simultaneous wireless information and power transfer
PLC	Power line communication
SG	Smart grids
IoT	Internet of Things
HWP	Hybrid wireless and power line communication
EE	Energy efficiency
SE	Spectrum efficiency
PT	Power transmission
PS	Power splitting
PSR	Power splitting-based relaying
TSR	Time splitting-based relaying
(O)DF	(Opportunistic) decode-and-forward
(O)AF	(Opportunistic) amplify-and-forward
ODF-AF	Opportunistic DF-AF
HD	Half-duplex
FD	Full-duplex
RS	Relay selection
SDP	Signal decision processor
SNR	Signal-to-noise ratio
CSI	Channel state information
AWGN	Additive white Gaussian noise
i.i.d.	independently and identically distributed
PDF	Probability density function
CDF	Cumulative distribution function
\mathcal{OP}	Outage probability
\mathcal{STP}	Successful transmission probability
ACK	Acknowledgement signal
RV	Random variable
TDMA	Time division multiple access
SC	Selection combining
S	The source node
D	The destination node
R_i	The i -th relay of K relays, ($1 \leq i \leq K$)
X, Y, Z	The channel coefficients of S-R _{i} , R _{i} -D, S-D links
$ X ^2, Y ^2$ and $ Z ^2$	The i.i.d. log-normal RVs with $LN(2\omega_X, 4\Omega_X^2)$, $LN(2\omega_Y, 4\Omega_Y^2)$ and $LN(2\omega_Z, 4\Omega_Z^2)$
ω_j, Ω_j^2	The mean and the standard deviation of $10 \log_{10}(j), j \in \{X; Y; Z\}$
d_X, d_Y, d_Z	The S-R _{i} , R _{i} -D, S-D distances
P_S	The power of S
P_{R_i}	The energy of i -th R
n_j	Additive white Gaussian noise (AWGN), ($j \in \{r_k, d\}$)
N_0	The zero mean and variance at the i -th R and D
χ_i	The decoding state of ODF-AF R _{i} , $i \in 1, \dots, K$

References

- Andrews, J.G.; Buzzi, S.; Choi, W.; Hanly, S.V.; Lozano, A.; Soong, A.C.K.; Zhang, J.C. What will 5G be? *IEEE J. Sel. Areas Commun.* **2014**, *32*, 1065–1082. [[CrossRef](#)]
- Osseiran, A.; Boccardi, F.; Braun, V.; Kusume, K.; Marsch, P.; Maternia, M.; Queseth, O.; Schellmann, M.; Schotten, H.; Taoka, H.; et al. Scenarios for 5G mobile and wireless communications: The vision of the METIS project. *IEEE Commun. Mag.* **2014**, *52*, 26–35. [[CrossRef](#)]
- Agiwal, M.; Roy, A.; Saxena, N. Next generation 5G wireless networks: A comprehensive survey. *IEEE Commun. Surv. Tutor.* **2016**, *18*, 1617–1655. [[CrossRef](#)]
- Palattella, M.R.; Dohler, M.; Grieco, A.; Rizzo, G.; Torsner, J.; Engel, T.; Ladid, L. Internet of Things in the 5G era: Enablers architecture and business models. *IEEE J. Sel. Areas Commun.* **2016**, *34*, 510–527. [[CrossRef](#)]
- Lin, J.; Yu, W.; Zhang, N.; Yang, X.; Zhang, H.; Zhao, W. A survey on Internet of Things: Architecture enabling technologies security privacy and applications. *IEEE Internet Things J.* **2017**, *4*, 1125–1142. [[CrossRef](#)]
- Nguyen, H.-S.; Voznak, M.; Nguyen, M.-T.; Sevcik, L. Performance Analysis with Wireless Power Transfer Constraint Policies in Full-Duplex Relaying Networks. *Elektronika ir Elektrotehnika* **2017**, *23*, 70–76. [[CrossRef](#)]
- Lu, X.; Wang, P.; Niyato, D.; Kim, D.I.; Han, Z. Wireless networks with RF energy harvesting: A contemporary survey. *IEEE Commun. Surv. Tutor.* **2015**, *17*, 757–789. [[CrossRef](#)]
- Huang, K.; Zhou, X. Cutting the last wires for mobile communications by microwave power transfer. *IEEE Commun. Mag.* **2015**, *53*, 86–93. [[CrossRef](#)]
- Ponnimbade Perera, T.D.; Jayakody, D.N.K.; Sharma, S.K.; Chatzinotas, S.; Li, J. Simultaneous Wireless Information and Power Transfer (SWIPT): Recent Advances and Future Challenges. *IEEE Commun. Surv. Tutor.* **2018**, *20*, 264–302. [[CrossRef](#)]
- Zhang, R.; Ho, C. MIMO broadcasting for simultaneous wireless information and power transfer. *IEEE Trans. Wirel. Commun.* **2013**, *12*, 1989–2001. [[CrossRef](#)]
- Zhou, X.; Zhang, R. Ho, C. Wireless information and power transfer: Architecture design and rate-energy tradeoff. *IEEE Trans. Commun.* **2013**, *61*, 4754–4767. [[CrossRef](#)]
- Liu, L.; Zhang, R.; Chua, K. Wireless Information Transfer with Opportunistic Energy Harvesting. *IEEE Trans. Wirel. Commun.* **2013**, *12*, 288–300. [[CrossRef](#)]
- Ng, D.W.K.; Lo, E.S.; Schober, R. Wireless Information and Power Transfer: Energy Efficiency Optimization in OFDMA Systems. *IEEE Trans. Wirel. Commun.* **2013**, *12*, 6352–6370. [[CrossRef](#)]
- Chang, Z.; Wang, Z.; Guo, X.; Yang, C.; Han, Z.; Ristaniemi, T. Distributed Resource Allocation for Energy Efficiency in OFDMA Multicell Networks With Wireless Power Transfer. *IEEE J. Sel. Areas Commun.* **2019**, *37*, 345–356. [[CrossRef](#)]
- Ng, D.W.K.; Schober, R. Dynamic resource allocation in OFDMA systems with full-duplex and hybrid relaying. In Proceedings of the 2011 IEEE International Conference on Communications (ICC), Kyoto, Japan, 5–9 June 2011; pp. 1–6.
- Zhang, M.; Liu, Y. Energy Harvesting for Physical-Layer Security in OFDMA Networks. *IEEE Trans. Inf. Forens. Secur.* **2016**, *11*, 154–162. [[CrossRef](#)]
- Yu, H.; Guo, S.; Yang, Y.; Ji, L.; Yang, Y. Secrecy Energy Efficiency Optimization for Downlink Two-User OFDMA Networks with SWIPT. *IEEE Syst. J.* **2019**, *13*, 324–335. [[CrossRef](#)]
- Nasir, A.A.; Zhou, X.; Durrani, S.; Kennedy, R.A. Relaying protocols for wireless energy harvesting and information processing. *IEEE Trans. Wirel. Commun.* **2013**, *12*, 3622–3636. [[CrossRef](#)]
- Nguyen, H.-S.; Nguyen, T.-S.; Voznak, M. Wireless powered D2D communications underlying cellular networks: Design and performance of the extended coverage. *Automatika* **2017**, *58*, 391–399. [[CrossRef](#)]
- Xia, M.; Assa, S. Modeling and analysis of cooperative relaying in spectrum-sharing cellular systems. *IEEE Trans. Veh. Technol.* **2016**, *65*, 9112–9122. [[CrossRef](#)]
- Chen, E.; Xia, M.; da Costa, D.B.; Assa, S. Multi-hop cooperative relaying with energy harvesting from cochannel interferences. *IET Commun.* **2017**, *21*, 1089–7798. [[CrossRef](#)]
- Laneman, J.N.; Tse, D.N.C.; Wornell, G.W. Cooperative diversity in wireless networks: Efficient protocols and outage behavior. *IEEE Trans. Inf. Theor.* **2004**, *50*, 3062–3080. [[CrossRef](#)]
- Bhatnagar, M.R.; Hjorungnes, A. ML decoder for decode-and-forward based cooperative communication system. *IEEE Trans. Wirel. Commun.* **2011**, *10*, 4080–4090. [[CrossRef](#)]
- Li, Y.; Vučetić, B. On the performance of a simple adaptive relaying protocol for wireless relay networks. In Proceedings of the VTC Spring 2008—IEEE Vehicular Technology Conference, Marina Bay, Singapore, 11–14 May 2008.
- Su, W.; Liu, X. On optimum selection relaying protocols in cooperative wireless networks. *IEEE Trans. Commun.* **2010**, *58*, 52–57. [[CrossRef](#)]
- Zhang, T.; Chen, W.; Cao, Z. Opportunistic DF-AF selection relaying with optimal relay selection in Nakagami-m fading environments. In Proceedings of the 2012 1st IEEE International Conference on Communications in China (ICCC), Beijing, China, 15–17 August 2012; pp. 619–624.
- Li, D. Opportunistic DF-AF Selection for Cognitive Relay Networks. *IEEE Trans. Veh. Technol.* **2016**, *65*, 2790–2796. [[CrossRef](#)]
- Xiuping, W.; Feng, Y.; Tian, Z. The DF-AF Selection Relay Transmission Based on Energy Harvesting. In Proceedings of the 10th International Conference on Measuring Technology and Mechatronics Automation (ICMTMA), Changsha, China, 10–11 February 2018; pp. 174–177.

29. Nguyen, H.-S.; Bui, A.; Do, D.; Voznak, M. Imperfect channel state information of AF and DF energy harvesting cooperative networks. *China Commun.* **2016**, *13*, 11–19. [[CrossRef](#)]
30. Riihonen, T.; Werner, S.; Wichman, R. Hybrid Full-Duplex/Half-Duplex Relaying with Transmit Power Adaptation. *IEEE Trans. Wirel. Commun.* **2011**, *10*, 3074–3085. [[CrossRef](#)]
31. Nguyen, H.-S.; Nguyen, T.-S.; Vo, V.-T.; Voznak, M. Hybrid full-duplex/half-duplex relay selection scheme with optimal power under individual power constraints and energy harvesting. *Comput. Commun.* **2018**, *124*, 31–44. [[CrossRef](#)]
32. Zhang, Z.; Chai, X.; Long, K.; Vasilakos, A.V.; Hanzo, L. Full duplex techniques for 5G networks: Self-interference cancellation, protocol design, and relay selection. *IEEE Commun. Mag.* **2015**, *53*, 128–137. [[CrossRef](#)]
33. Foschini, G.J. Layered space-time architecture for wireless communication in a fading environment when using multi-element antennas. *Bell Syst. Technol. J.* **1996**, *1*, 41–59. [[CrossRef](#)]
34. Krikidis, I.; Suraweera, H.A.; Smith, P.J.; Yuen, C. Full-Duplex Relay Selection for Amplify-and-Forward Cooperative Networks. *IEEE Trans. Wirel. Commun.* **2012**, *11*, 4381–4393. [[CrossRef](#)]
35. Luo, S.; Teh, K.C. Buffer State Based Relay Selection for Buffer-Aided Cooperative Relaying Systems. *IEEE Trans. Wirel. Commun.* **2015**, *14*, 5430–5439. [[CrossRef](#)]
36. Zou, Y.; Champagne, B.; Zhu, W.; Hanzo, L. Relay-Selection Improves the Security-Reliability Trade-Off in Cognitive Radio Systems. *IEEE Trans. Commun.* **2015**, *63*, 215–228. [[CrossRef](#)]
37. Wang, W.; Teh, K.C.; Li, K.H. Generalized Relay Selection for Improved Security in Cooperative DF Relay Networks. *IEEE Wirel. Commun. Lett.* **2016**, *5*, 28–31. [[CrossRef](#)]
38. Oestges, C.; Czink, N.; Bandemer, B.; Paulraj, A. Capacity performance of outdoor-to-indoor relay schemes in measured radio channels. In Proceedings of the IEEE 20th International Symposium on Personal, Indoor and Mobile Radio Communications, Tokyo, Japan, 13–16 September 2009; pp. 1113–1117.
39. Renzo, M.D.; Graziosi, F.; Santucci, F. A comprehensive framework for performance analysis of cooperative multi-hop wireless systems over log-normal fading channels. *IEEE Trans. Commun.* **2010**, *58*, 531–544. [[CrossRef](#)]
40. Nouri, H.; Touati, F.; Uysal, M. Diversity-Multiplexing Tradeoff for Log-Normal Fading Channels. *IEEE Trans. Commun.* **2016**, *64*, 3119–3129. [[CrossRef](#)]
41. Zhu, B.; Cheng, J.; Yan, J.; Wang, J.; Wu, L.; Wang, Y. A new technique for analyzing asymptotic outage performance of diversity over log-normal fading channels. In Proceedings of the 15th Canadian Workshop on Information Theory (CWIT), Quebec City, QC, Canada, 11–14 June 2017; pp. 1–5.
42. Cammin, C.; Krush, D.; Heynicke, R.; Scholl, G. Test method for narrowband F/TDMA-based wireless sensor/actuator networks including radio channel emulation in severe multipath environments. *J. Sens. Sens. Syst.* **2018**, *7*, 183–192. [[CrossRef](#)]
43. Liu, Y.; Xiao, R.; Shen, J.; Yang, H.; Yan, C. Hybrid protocol for wireless energy harvesting network over log-normal fading channel. *J. Eng.* **2018**, *6*, 339–341. [[CrossRef](#)]
44. Liu, Y.; Shen, J.; Pan, Z.; Xiao, R.; Yang, H.; Yan, C. Performance analysis of dual-hop AF relaying networks over log-normal fading channels with interferences. In Proceedings of the IEEE/CIC International Conference on Communications Workshops in China (ICCC Workshops), Changchun, China, 1–13 August 2019; pp. 130–135.
45. Rabie, K.; Tonello, A.M.; Al-Dhahir, N.; Song, J.; Sendin, A. IEEE Access Special Section Editorial: Advances in Power Line Communication and its Applications. *IEEE Access* **2019**, *7*, 133371–133374. [[CrossRef](#)]
46. Rubin, I.; Lin, Y.; Kofman, D. Relay-aided networking for power line communications. In Proceedings of the 2014 Information Theory and Applications Workshop (ITA), San Diego, CA, USA, 9–14 February 2014; pp. 1–6.
47. Qian, Y.; Yan, J.; Guan, H.; Li, J.; Zhou, X.; Guo, S.; Jayakody, D.N.K. Design of Hybrid Wireless and Power Line Sensor Networks With Dual-Interface Relay in IoT. *IEEE Internet Things J.* **2019**, *6*, 239–249. [[CrossRef](#)]
48. Lee, J.; Kim, Y. Diversity Relaying for Parallel Use of Power-Line and Wireless Communication Networks. *IEEE Trans. Power Deliv.* **2014**, *29*, 1301–1310. [[CrossRef](#)]
49. Dib, L.d.M.B.A.; Fernandes, V.; Filomeno, M.d.L.; Ribeiro, M.V. Hybrid PLC/Wireless Communication for Smart Grids and Internet of Things Applications. *IEEE Internet Things J.* **2018**, *5*, 655–667. [[CrossRef](#)]
50. Rabie, K.M.; Adebisi, B.; Yousif, E.H.G.; Gacanin, H.; Tonello, A.M. A comparison between orthogonal and non-orthogonal multiple access in cooperative relaying power line communication systems. *IEEE Access* **2017**, *5*, 10118–10129. [[CrossRef](#)]
51. Pu, H.; Liu, X.; Zhang, S.; Xu, D. Adaptive cooperative non-orthogonal multiple access-based power line communication. *IEEE Access* **2019**, *7*, 73856–73869. [[CrossRef](#)]
52. Ahiadormey, R.K.; Anokye, P.; Lee, K.-J. Cooperative non-orthogonal multiple access over log-normal power line communication channels. *Electronics* **2019**, *8*, 1254. [[CrossRef](#)]
53. Ahiadormey, R.K.; Anokye, P.; Park, S.-H.; Lee, K.-J. Two-Way Relaying Non-Orthogonal Multiple Access with Imperfect Successive Interference Cancellation in Power Line Communications. *IEEE Open J. Commun. Soc.* **2020**, *1*, 1872–1885. [[CrossRef](#)]
54. Bletsas, A.; Khisti, A.; Reed, D.; Lippman, A. A simple cooperative diversity method based on network path selection. *IEEE J. Sel. Areas Commun.* **2006**, *24*, 659–672. [[CrossRef](#)]
55. Wang, H.; Ma, S.; Ng, T.-S.; Poor, H.V. A general analytical approach for opportunistic cooperative systems with spatially random relays. *IEEE Trans. Wirel. Commun.* **2011**, *10*, 4122–4129. [[CrossRef](#)]
56. Nasir, A.A.; Zhou, X.; Durran, S.; Kennedy, R.A. Wireless-Powered Relays in Cooperative Communications: Time-Switching Relaying Protocols and Throughput Analysis. *IEEE Trans. Commun.* **2015**, *63*, 1607–1622. [[CrossRef](#)]